IOPscience iopscience.iop.org

Home Search Collections Journals About Contact us My IOPscience

Structural and optical properties of In-rich InGaN nanodots grown by metallo-organic chemical vapor deposition

This content has been downloaded from IOPscience. Please scroll down to see the full text.

2007 Nanotechnology 18 405305

(http://iopscience.iop.org/0957-4484/18/40/405305)

View the table of contents for this issue, or go to the journal homepage for more

Download details:

IP Address: 140.113.38.11

This content was downloaded on 26/04/2014 at 03:53

Please note that terms and conditions apply.

Nanotechnology 18 (2007) 405305 (4pp) doi:10.1088/0957-4484/18/40/405305

Structural and optical properties of In-rich InGaN nanodots grown by metallo-organic chemical vapor deposition

Wen-Che Tsai, Hsuan Lin, Wen-Chen Ke, Wen-Hao Chang[1], Wu-Ching Chou, Wei-Kuo Chen and Ming-Chih Lee[1]

Department of Electrophysics, National Chiao Tung University, Hsinchu 300, Taiwan

E-mail: whchang@mail.nctu.edu.tw and mclee@cc.nctu.edu.tw

Received 22 May 2007, in final form 19 July 2007
Published 17 September 2007
Online at stacks.iop.org/Nano/18/405305

Abstract
The surface morphologies, alloy compositions and emission properties of In-rich $In_xGa_{1-x}N$ nanodots ($x \geqslant 0.87$) grown by metallo-organic chemical vapor deposition at various growth temperatures (550–750 °C) were investigated. We found that the nucleation of InGaN dots was dominated by the surface migration of In adatoms. A higher Ga content can be achieved at lower growth temperatures due to the relatively lower migration ability of Ga adatoms. At higher growth temperatures, the InGaN dots tend to decompose into In-rich islands and a thin Ga-rich layer. These In-rich islands exhibit photoluminescence emission in the near-infrared range. Another visible emission band was also observed for samples grown at higher temperatures. The formation of a thin Ga-rich layer is likely to be responsible for the visible emission.

(Some figures in this article are in colour only in the electronic version)

1. Introduction

Group-III nitrides have become the most promising materials for a variety of optoelectronic devices [1]. Of particular importance are heterostructures incorporating ternary InGaN alloys, which have been used as active materials in commercial light-emitting diodes (LEDs) and laser diodes operating in the blue-green and ultraviolet spectral ranges [2]. Recently, many experimental evidences have shown that the energy gap of InN is around 0.7 eV [3, 4], rather than the previously accepted value of 1.9 eV. This finding has stimulated considerable interest, since the potential application of ternary InGaN alloys can be further extended into the near-infrared (NIR) range. However, the growth of InGaN alloys, particularly with high In content, remains a great challenge. The difficulty arises not only from the high vapor pressure of N_2 over InN [5], but also from the large lattice mismatch between InN and GaN (∼11%). In particular, it has been theoretically predicted that InGaN alloys are thermodynamically unstable and show a miscibility gap in the phase diagram at typical growth temperatures [6]. Although the growth processes taking place in epitaxial methods like metallo-organic chemical vapor deposition (MOCVD) and molecular beam epitaxy are mostly nonequilibrium ones, phase separations and composition fluctuations are still commonly observed in InGaN thick films [7, 8] as well as InGaN/GaN quantum wells [8, 9]. In the last decade, nanoscale In-rich regions formed by local compositional fluctuations in InGaN alloys have been intensively investigated, because such nanostructures were believed to act as 'quantum dots' for localizing carriers and were considered to play a key role in the high radiative efficiency of InGaN-based LEDs [10, 11]. In this context, self-assembled island growth of InGaN/GaN dots appears to be a more controllable way for realizing such In-rich nanostructures [12–15]. However, the $In_xGa_{1-x}N$ dots reported to date are still on the Ga-rich side ($x < 0.5$), with typical emission wavelength in the blue-green range. On the In-rich side ($0.5 < x < 1$), the study of $In_xGa_{1-x}N$ dots with NIR emissions is still absent.

Recently, we have demonstrated that InN/GaN nanodots formed during the initial stage of heteroepitaxial growth using

[1] Authors to whom any correspondence should be addressed.

 © 2007 IOP Publishing Ltd Printed in the UK

MOCVD can exhibit intense photoluminescence emissions in the NIR range [16, 17]. In this paper, we further investigate In-rich $In_xGa_{1-x}N$ nanodots (with $x > 0.87$) grown at various temperatures by MOCVD. Atomic force microscopy (AFM), x-ray diffraction (XRD), photoluminescence (PL) measurements and near-field scanning optical microscopy (NSOM) are employed to study the correlation among surface morphologies, alloy compositions and PL emission bands of these In-rich $In_xGa_{1-x}N$ dots.

2. Experimental details

The uncapped InGaN nanodots samples were grown on sapphire (0001) by MOCVD using trimethylgallium (TMGa), trimethylindium (TMIn), and NH_3 as source materials. After the growth of a 2 μm thick undoped GaN buffer layer at 1120 °C, the substrate temperature was decreased to 550–750 °C to grow InGaN dots using modulated precursor injection schemes. The precursor flow rates were 1, 150 and 18 000 SCCM (SCCM denotes cubic centimeter per minute at standard temperature and pressure, STP) for the TMGa, TMIn and NH_3, respectively. The details of the gas flow sequence have been reported in [17]. The only difference is that a 1 SCCM TMGa flow was supplied concurrently with the TMIn flow to grow InGaN alloys. During the TMGa and TMIn flow periods, the NH_3 background flow rate was controlled at 10 000 SCCM. PL measurements were carried out at $T = 10$ K using the 325 nm line of a He–Cd laser as an excitation source. The PL signals were analyzed by a 0.5 m monochromator and detected by either a photomultiplier tube or a cooled extended InGaAs detector (with a cutoff wavelength at 2.05 μm) for the visible and NIR spectral ranges, respectively. For NSOM measurements, a fiber tip was mounted on the tuning fork of an AFM system for simultaneous measurement of the surface morphology and emission signal using the illumination–collection mode. The tip–sample distance was kept at ∼30 nm, and was controlled by the shear-force feedback mechanism.

3. Results and discussion

The surface morphologies of InGaN dots were studied by AFM. The sample grown at 550 °C shows a rough film formed by coalescent islands. For growth temperatures in the range $T_g = 600$–725 °C, individual InGaN dots were observed, which are shown in figure 1(a). With increasing T_g, the average height and diameter of the InGaN dots increased from 24 to 114 nm and 75 to 410 nm, respectively, whereas the dot density decreased from 4.0×10^9 to 2.2×10^7 cm^{-2}. The dot density as a function of T_g is depicted in figure 1(b). In the range $T_g = 600$–700 °C, the decreasing dot density with increasing T_g can be attributed to the enhanced migration length of adatoms, resulting in much larger and less dense dots at higher growth temperatures [17]. For $T_g > 700$ °C, the dot density decreased rapidly and dropped to zero at 750 °C, due possibly to the desorption of metallic In from the growing surface. To further study the nucleation mechanism of InGaN dots, we also prepared a series of samples with InN dots grown at different T_g under similar growth conditions. The density of InN dots as a function of T_g is also included in

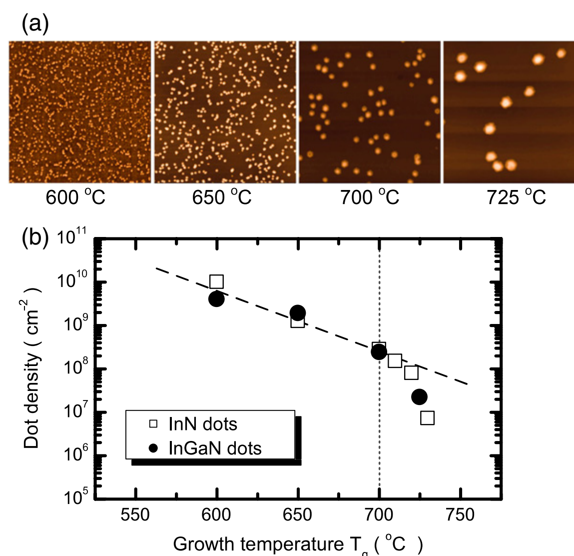

Figure 1. (a) AFM morphology of InGaN dots grown at different temperatures. The images shown are in an area of 5×5 μm^2. (b) The dot density as a function of growth temperature.

figure 1(b). We found that the densities of InGaN and InN dots show a similar dependence on T_g, implying that the nucleation of InGaN dots is governed by the surface migration of In adatoms, rather than Ga or both. This can be realized from the very different migration capabilities of In and Ga adatoms on the GaN surface. Since the bond strength of InN (7.7 eV/atom) is weaker than that of GaN (8.9 eV/atom), In adatoms (or its adsorbed precursor molecules) are expected to have a considerably longer migration length on the GaN surface, leading to a much higher nucleation rate and hence governing the formation of InGaN dots.

The In compositions of the InGaN dots were determined by XRD. Figure 2 shows XRD θ–2θ scans of the investigated samples near the InN(0002) and GaN(0002) diffraction peaks. A diffraction curve of InN film grown on GaN is also included. For the InGaN samples, a broad diffraction peak corresponding to ternary InGaN dots was found to shift gradually toward the InN(0002) peak as T_g was increased from 550 to 725 °C. For the sample grown at 750 °C, the InGaN peak disappeared, due to the complete desorption of In from the growing surface. Using Vegard's law, we have estimated that the In content (x) of the $In_xGa_{1-x}N$ dots increases from 0.87 to 0.99 as T_g is increased from 550 to 725 °C. This increasing trend is also a consequence of the lower diffusion ability of Ga adatoms. At lower T_g, the growth is under the kinetic-dominant condition, so Ga incorporation at island sites could be more dominant. With increasing T_g, the growth conditions become closer to the thermodynamic conditions, which allows the Ga adatoms to select thermodynamically more stable sites and hence hinders the incorporation of Ga adatoms into the In-rich islands. This can be seen from the case of $T_g = 725$ °C: the $In_xGa_{1-x}N$ dots become highly In-rich, with x up to 0.99. Therefore, it can be inferred that most of the deposited Ga adatoms are distributed among these In-rich islands, forming a thin Ga-rich layer. We would like to point out that the deduced In content from figure 2 does not follow the prediction of equilibrium solubility

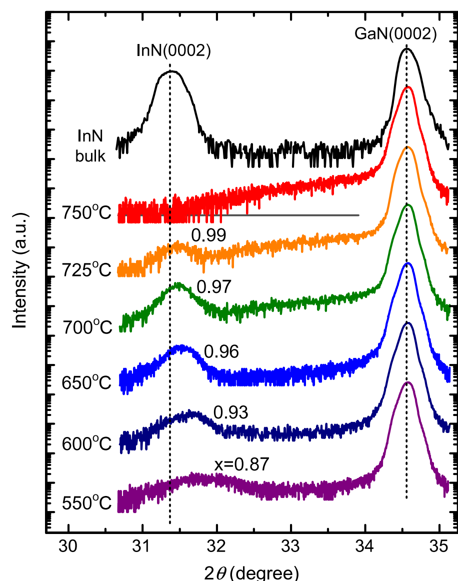

Figure 2. X-ray diffraction of InGaN dots grown at different temperatures.

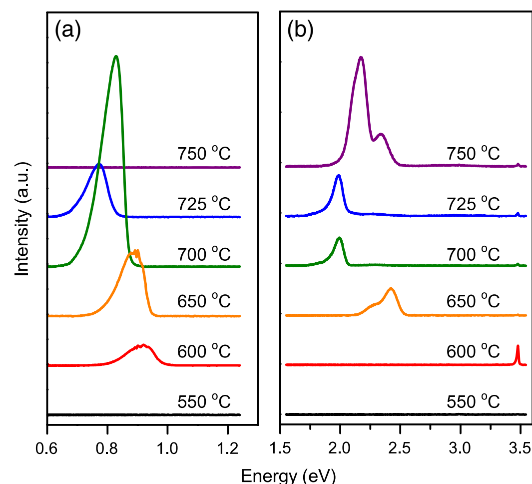

Figure 3. Photoluminescence spectra of InGaN dots grown at different temperatures from 550 to 750 °C in (a) the NIR and (b) the visible spectral ranges.

of GaN in InN based on thermodynamic considerations [6], where the Ga content is expected to increase with the growth temperature. For example, in [6], the solubility of GaN in InN is predicted to be 3% at 550 °C and 6% at 725 °C, while our result shows 13% at 550 °C and about 1% at 725 °C. This clearly indicates that the incorporation of Ga into InN during the growth of InGaN dots is affected by the surface kinetics of In and Ga adatoms, rather than equilibrium solubility.

The optical properties of these In-rich InGaN dots were studied by PL measurements. Both the visible and the NIR spectral ranges were investigated; they are shown in figures 3(a) and (b), respectively. No PL signal was observed for the 550 °C grown sample, since low-temperature growth is detrimental to their optical quality. Samples grown at T_g = 600–725 °C exhibit an NIR emission band in the range of 0.77–0.92 eV. A clear redshift in the PL peak energy with increasing T_g can be seen. Since these nanodots are rather large, the energy shift caused by the variation in dot size was estimated to be less than 15 meV, which cannot account for the observed total shift of about 150 meV. Therefore, differences in peak energy between samples must come mainly from the variations of the alloy composition in InGaN dots. In fact, the PL peak energy agrees fairly well with the corresponding In content determined by XRD. Accordingly, we identify the NIR band as the emission from In-rich InGaN dots. For the sample grown at 750 °C, the NIR band disappeared due to the absence of In-rich islands, which is also consistent with its surface morphology and XRD data. Apart from the NIR band, we also observed a visible emission band in the range of 2.0–2.4 eV for samples grown at $T_g \geqslant$ 650 °C. Significantly, the visible emission is even stronger for the sample grown at T_g = 750 °C, in spite of the absence of In-rich islands, implying that the visible band does not originate from the InGaN dots. To further clarify this point, we performed NSOM measurements at room temperature to obtain both the surface morphology and the spatial distribution of visible emissions. Figure 4(a) shows such an NSOM image of the 725 °C sample, mapping at its visible emission peak. The corresponding surface morphology is shown in figure 4(b). It can be clearly seen that these two images are nearly complementary, with dark spots in the NSOM image corresponding very well with the In-rich islands revealed in the AFM image. This confirms that the visible emission does indeed originate from the 'flat region' outside these In-rich islands. As can be seen from figure 4(a), the visible emission is mainly contributed by some bright spots located among these In-rich islands. As mentioned above, the deposited Ga atoms during the growth of InGaN dots may form a thin Ga-rich layer among these In-rich islands, due to the considerably shorter migration length for Ga adatoms. The visible emission band may originate from defect centers induced during the formation of the Ga-rich layer.

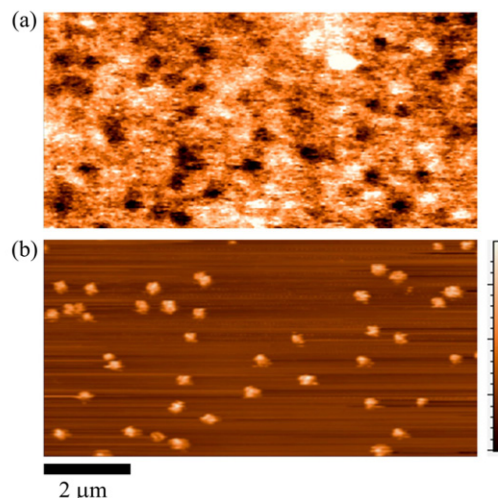

Figure 4. (a) NSOM image of the 725 °C grown sample mapping at its visible emission peak at room temperature. (b) The corresponding AFM image.

4. Conclusion

In summary, the surface morphologies, alloy compositions and PL properties of In-rich InGaN nanodots grown by MOCVD at $T_g = 550$–$750\,^{\circ}\mathrm{C}$ have been investigated. The nucleation of InGaN dots was found to be dominated by the surface migration of In adatoms. In particular, we found that the incorporation of Ga into InN during the growth of InGaN dots is governed by the adatom migration capability, which tends to decompose into In-rich islands and a thin Ga-rich layer at higher growth temperatures. In-rich islands exhibit PL emission in the NIR range, while the formation of a thin Ga-rich layer is likely to be responsible for the observed visible emission band.

Acknowledgments

This work is supported in part by the project of MOE-ATU and the National Science Council of Taiwan under grant Nos NSC 95-2112-M-009-047, NSC 95-2112-M-009-012, NSC 95-2112-M-009-044-MY3, and NSC 95-2112-M-009-020.

References

[1] See for review Gil B (ed) 1998 *Group III Nitride Semiconductor Compounds* (Oxford: Clarendon)
[2] Nakamura S and Fasol G 1997 *The Blue Laser Diode* (Berlin: Springer)
[3] Davydov V Yu *et al* 2002 *Phys. Status Solidi* b **229** R1
[4] Wu J, Walukiewicz W, Yu K M, Ager J W III, Haller E E, Lu H, Schaff W J, Saito Y and Nanishi Y 2002 *Appl. Phys. Lett.* **80** 3967
[5] Bhuiyan A G, Hashimoto A and Yamamoto A 2003 *J. Appl. Phys.* **94** 2779
[6] Ho I and Stringfellow G B 1996 *Appl. Phys. Lett.* **69** 2701
[7] Singh R, Doppalapudi D, Moustakas T D and Romano L T 1997 *Appl. Phys. Lett.* **70** 1089
[8] El-Masry N A, Piner E L, Liu S X and Bedair S M 1998 *Appl. Phys. Lett.* **72** 40
[9] Chichibu S, Wada K and Nakamura S 1997 *Appl. Phys. Lett.* **71** 2346
[10] Nakamura S 1998 *Science* **281** 956
[11] O'Donnell K P, Martin R W and Middleton P G 1999 *Phys. Rev. Lett.* **82** 237
[12] Hirayama H, Tanaka S, Ramvall P and Aoyagi Y 1998 *Appl. Phys. Lett.* **72** 1736
[13] Tachibana K, Someya T and Arakawa Y 1999 *Appl. Phys. Lett.* **74** 383
[14] Damilano B, Grandjean N, Dalmasso S and Massies J 1999 *Appl. Phys. Lett.* **75** 3751
[15] Adelmann C, Simon J, Feuillet G, Pelekanos N T, Daudin B and Fishman G 2000 *Appl. Phys. Lett.* **76** 1570
[16] Ke W C *et al* 2006 *Appl. Phys. Lett.* **88** 191913
[17] Ke W C, Lee L, Chen C Y, Tsai W C, Chang W-H, Chou W C, Lee M C, Chen W K, Lin W J and Cheng Y C 2006 *Appl. Phys. Lett.* **89** 263117